Structure-Activity Relationship within a new series of σ_1 and σ_2 receptor ligands: identification of a novel σ_2R agonist (BS148) with selective toxicity against metastatic melanoma

Silvia Franchini,[a] Claudia Sorbi,[a] Battisti Umberto Maria,[a] Annalisa Tait,[a] Leda Ivanova Bencheva,[a] Elena Cichero,[b] Paola Fossa,[b] Antonio Cilia,[c] Orazio Prezzavento,[d] Simone Ronsisvalle,[d] Giuseppina Aricò,[d] Luisa Benassi,[e] Cristina Vaschieri,[e] Paola Azzoni,[e] Cristina Magnoni[e] and Livio Brasili[a]*

[a] Dipartimento di Scienze della Vita, Università degli Studi di Modena e Reggio Emilia, Via Campi 103, 41125 Modena, Italy.

[b] Dipartimento di Farmacia, Università degli Studi di Genova, Viale Benedetto XV 3, 16132 Genova, Italy.

[c] Divisione Ricerca e Sviluppo, Recordati S.p.A., Via Civitali 1, 20148 Milano, Italy

[d] Dipartimento di Scienze del Farmaco , Università degli Studi di Catania, Viale Andrea Doria 6, 95125, Catania, Italy

[e] Dipartimento Chirurgico, Medico, Odontoiatrico e di Scienze Morfologiche con interesse Trapiantologico, Oncologico e di Medicina Rigenerativa, Università degli Studi di Modena e Reggio Emilia, via del Pozzo 71, 41124 Modena, Italy.

Corresponding Author: Phone: +39 (0)59 2058584; E-mail: livio.brasili@unimore.it

Key words: Sigma receptors, Analgesia; Antiproliferative activity; Melanoma; SK-MEL-2 cell line.

Abstract

A new series of spiro-cyclic sigma ligands were prepared and studied. Most were found to have a high affinity and selectivity for σ_1R; compounds **7b, 15b** and **16a** were shown to be σ_1R agonists, while **16b** was proven to be the only σ_1R antagonist. Only **16a** (BS148) exhibited σ_2R selectivity and was able to inhibit the growth of metastatic malignant melanoma cell lines, whilst not affecting normal human melanocytes. BS148's anti-proliferative activity suggests a σ_2R agonist profile. Further, preliminary investigations indicate that, at least a part, the mechanism of metastatic malignant melanoma cell death induced by BS148 is due to apoptosis.

Introduction

Sigma receptors (σRs), initially classified as an additional class of opioid receptors,[1] are nowadays considered a unique entity with no homology to opioid receptors or other mammalian proteins.[2] After its discovery radioligand binding studies and biochemical analysis classified sigma receptors as two different and distinct subtypes, sigma-1 (σ_1R) and sigma-2 (σ_2R).[3,4]

The σ_1R has been characterized and cloned from different species, including humans.[5-9] It has been shown that the endogenous regulators progesterone, dehydroepiandrosterone, N,N-dimethyltryptamine[10-12] and several exogenous ligands such as benzomorphans (SKF10047 and pentazocine),[13-17] haloperidol and NE-100 can interact with the σ_1R.[14, 17-19] High affinity σ_1R ligands have been considered to play an important role in the treatment of various neurodegenerative disorders including Parkinson's, Alzheimer's and Huntington's disease, dementias, cognitive aging, depression, schizophrenia, neuropathic pain, drug addiction, stroke, HIV infection and cancer.[20-29] Unlike σ_1Rs, σ_2Rs are less understood and have not yet been cloned. Recently, the progesterone receptor membrane component 1 (PGRMC1) has been proposed as the σ_2R binding site,[30] although this was questioned by other evidence supporting that the two target are two different proteins.[31] More recently TMEM97, an endoplasmic reticulum (ER)-resident membrane protein, possesses the full suite of molecular properties that define the σ_2 receptor.[32] Activation of σ_2R appears to be involved in the regulation of cellular proliferation and cell death.[33,34] Furthermore, it has been reported that σ_2R ligands can be used as biomarkers in various rapid proliferating tumors and thus they could be exploited for tumor imaging.[33,35] σ_1R and σ_2R have been found to be overexpressed in a variety of cancer cells[34] and it has been described that selective σ_1R antagonists and σ_2R agonists are able to modulate cancer cell viability and growth potential.[36,37] Among different types of cancer, metastatic malignant melanoma is by

far one of the most common and aggressive types, with approximately 76,000 new cases diagnosed and over 9,000 estimated deaths in 2013 in United States alone. Advanced-stage melanoma is often associated with an overall median survival period of 2-8 months and with only 5% of patients surviving beyond 5 years. At present, only three molecules have been approved by the US Food and Drug Administration (FDA) for the treatment of malignant metastatic melanoma: dacarbazine (DTIC), interleukin-2 (IL-2), and vemurafenib (Zelforab). Zelforab is the only molecule proven to be capable of increasing overall patient survival with low remission rates.[38]

Due to the broad diagnostic and therapeutic potential, the development of potent and selective σ_1R or σ_2R ligands is one of the primary challenges in medicinal chemistry. We recently reported a new series of conformationally restricted spiro-dioxolane among which **1a** and **1b** showed high affinity and good selectivity for σ_1R, behaving as σ_1R agonists (Figure 1).[39] Spirocyclic substructure have been shown to be an interesting moiety for σR ligands.[40, 41]

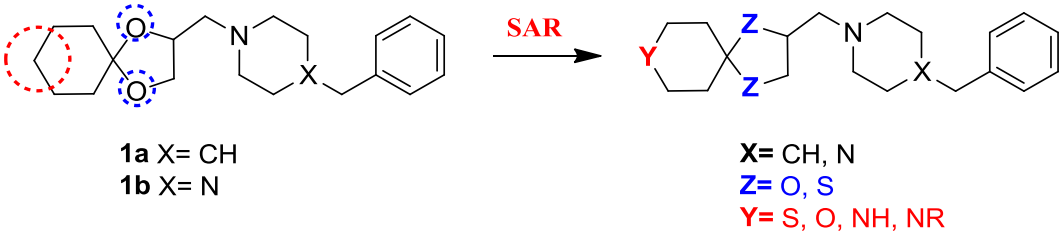

Figure 1. SAR studies on conformationally restricted spiro-dioxolane **1a** and **1b.**

In the present study, we explored a new set of structural related analogues of **1a** and **1b** in order to investigate the effect of different substitutions on both affinity and selectivity at σ_1R and σ_2R in an attempt to identify novel and selective ligands (Figure 1). The C8 position of the 1,4-dioxa-spiro[4.5]decane moiety was selected as a starting point, due to its feasible chemistry and because it could be exploited without adding a second stereogenic center. Thus, several substituents were introduced at position 8: H-bond donor/acceptor groups that

could establish H-bond contacts, aromatic group that might be beneficial for additional Van der Waals and π–π stacking, and bulky groups that could be favorable detecting hydrophobic contacts. Furthermore we generated variants of the leads, focusing our attention on the 1,3-dioxolane moiety, replacing it with the corresponding oxathiolane and dithiolane isosters. This approach led to extensive qualitative structure-activity relationship studies and the identification of valuable high affinity σR ligands. Docking studies were performed on the X-Ray crystallographic structure of the human σ_1R.

Results and Discussion

Chemistry

The synthetic strategy is described in Scheme 1 and 2.

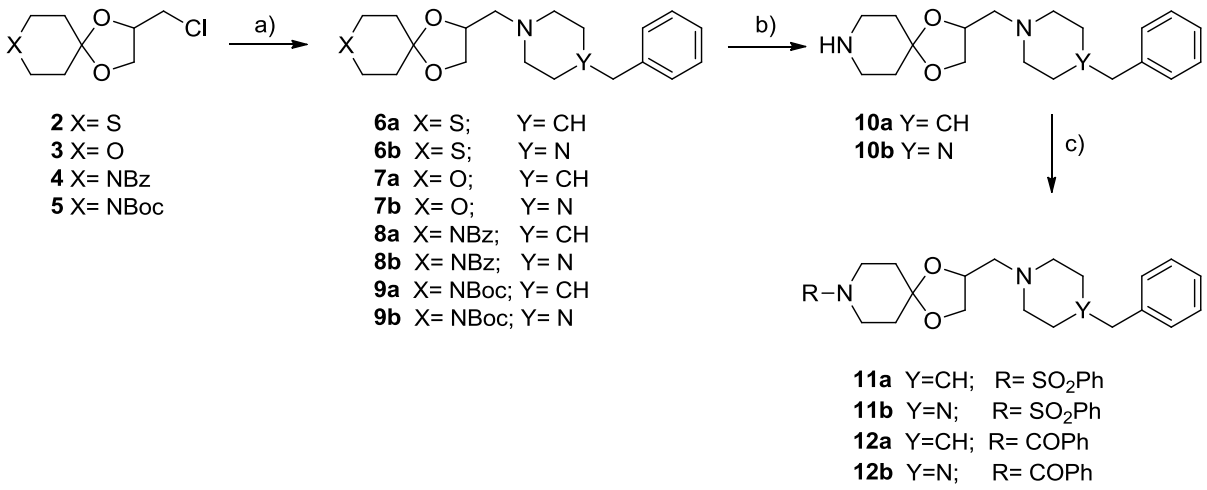

Scheme 1. Reagents and conditions: a) 4-benzylpiperidine or 1-benzylpiperazine, KI, 2-methoxyethanol, 120 °C, 12 h, 70% for **6a**, 85% for **6b**, 86% for **7a**, 58% for **7b**, 82% for **8a**, 77% for **8b**, 40% for **9a**, 27% for **9b**; b) TFA, CH_2Cl_2, 0 °C to 25 °C, 3 h, 93% for **10a**, 43% for **10b**; c) $C_6H_5SO_2Cl$ or C_6H_5COCl, Et_3N, CH_2Cl_2, 0 °C to 25 °C, 12 h, 32% for **11a**, 67% for **11b**, 57% for **12a**, 73% for **12b**.

The 1,3-dioxolane derivatives **2-5** were prepared as previously described[42] and reacted with 4-benzylpiperidine or 1-benzylpiperazine, under basic conditions, to yield compounds **6a**-**9a** and **6b**-**9b**. Furthermore, deprotection of **9a** and **9b**, with TFA, afforded the corresponding free amines **10a** and **10b**. Alkylation of their secondary aminic group with benzenesulfonyl chloride and/or benzoyl chloride gave compounds **11a**, **12a** and **11b**, **12b,** respectively.

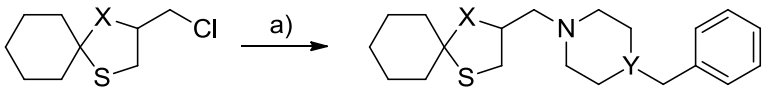

13 X= O; L= OTs
14 X= S; L= Cl

15a X= O; Y= CH
15b X= O; Y= N
16a X= S; Y= CH
16b X= S; Y= N

Scheme 2. Reagents and conditions: a) 4-benzylpiperidine or 1-benzylpiperazine, KI, 2-metoxyethanol, MW, 160 °C, 30 min, 65% for **15a**, 79% for **15b**, 28% for 1**6a**, 69% for 1**6b**.

The compounds **15a**, **16a** (BS148) and **15b**, **16b** were similarly prepared as outlined in Scheme 2, from the tosylate **13** or chloride **14**,[43] which were reacted with 4-benzylpiperidine or 1-benzylpiperazine to give full assignments of protons and carbons for all the compounds. This was done by ^{1}H and ^{13}C NMR analysis, through related 1D spectra acquisition and the study of key values obtained from ^{1}H-^{1}H COSY, ^{1}H-^{13}C HSQC and HMBC experiments. All final compounds were converted into oxalate salts using oxalic acid in acetone. The purities of the salts were confirmed by elemental analysis and the values obtained were within ±0.4% of the calculated ones. The exact mass of the salts was confirmed by HPLC-QTOF measurement.

Pharmacology

σ-Receptors binding affinities

All compounds were evaluated for their binding affinity at σ_1, σ_2, $5HT_{1A}$ and α_1 adrenoceptors (Table 1 and 2). The $5\text{-}HT_{1A}$ and α_1 adrenoceptors were investigated because most of the molecules share some chemical features with previously published $5\text{-}HT_{1A}R$ and α_1 ligands.[43-46] None of the compounds were found to bind to the α_1 adrenoceptors and therefore these data were not included in the Tables. Compounds **1a** and **1b**, were included as reference compounds in order to better understand the structure-affinity relationship. As previously reported, **1a** and **1b** bind preferentially to the σ_1R, with a 10- and 47-fold preference for σ_1R compared to the σ_2R, respectively. Isosteric substitution of the carbon atom at position 8 of the 1,4-dioxaspiro[4.5]decane with sulphur, oxygen or nitrogen atoms was initially studied. Increasing the polarity on 4-benzylpiperidine derivatives (**6a**<**7a**<**10a**) was shown to have a limited effect on both σ_1R and σ_2R affinity. **10a**, the most polar of the compounds, was the only compound to show a marked decrease in affinity for both σ_1R and σ_2R with a reverse σ_1/σ_2 selectivity. The observed decreased affinity is probably due to the protonation of the nitrogen atom and this positive charge seems to be an unfavorable factor for binding.

Table 1. Affinity constant (pK_i) and selectivity of the benzylpiperidine derivatives **6-12a**, **15-16a** and the reference compound **1a** at σ_1R, σ_2R and $5\text{-}HT_{1A}R$.

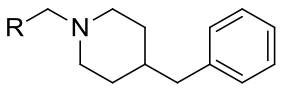

Comp.	R	$pK_i\sigma_1$ [a,b]	$pK_i\sigma_2$ [a,c]	σ_1/σ_2 [d]	pK_i5HT_{1A} [e]	$\sigma/5HT_{1A}$ [f]
1a	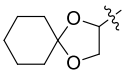	8.70	7.72	9.5	6.79	81

6a	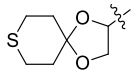	8.51	8.03	3	7.00	32
7a	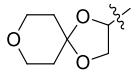	8.79	7.53	18	<6	>62
8a	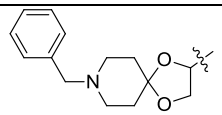	9.06	8.10	9	<6	>1150
9a	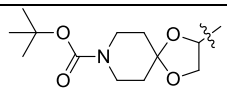	8.19	7.51	4.8	<6	>155
10a	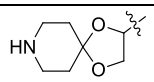	6.59	6.90	0.5	<6	>4
11a	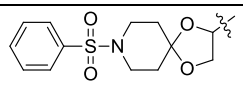	8.32	7.62	5	<6	>209
12a	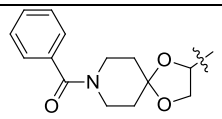	7.28	7	2	<6	>19
15a	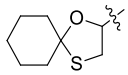	7.96	7.23	5.4	6.65	20
16a BS148	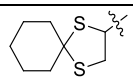	6.27	7.71	0.04	7	5

[a] K_i values agreed to ± 20%. [b] Binding assays were performed using 3.0 nM [^{3}H]pentazocine. [c] Binding assays were performed using 3.0 nM [^{3}H]ditolylguanidine. [d] Antilog of the difference between the pK_i values for σ_1 and σ_2 receptors. [e] K_i values were derived from the Cheng–Prusoff equation[47] at one or two concentrations and agreed within 10%. [f] Antilog of the difference between the pK_i values for σ receptors (higher value) and the 5-HT_{1A}R.

For 1-benzylpiperazine derivatives the increasing of polarity (**6b**<**7b**<**10b**) has even a stronger effect on affinity at σ_1R and σ_2R and compound **10b** is practically not able to bind at both receptors.

Table 2. Affinity constant (pK_i) and selectivity of the benzylpiperazine derivatives **6-12b**, **15-16b** and the reference compound **1b** at σ_1R, σ_2R and 5-HT_{1A}R.

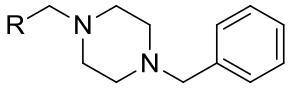

Comp.	R	$pK_i\sigma_1$ [a,b]	$pK_i\sigma_2$ [a,c]	σ_1/σ_2 [d]	pK_i5HT_{1A} [e]	$\sigma/5HT_{1A}$ [f]
1b	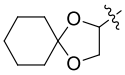	9.13	7.46	47	<6	>1349
6b	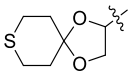	8.46	7.05	26	6.45	102
7b	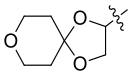	7.62	6.46	15	<6	>42
8b	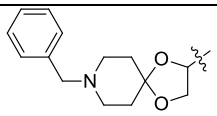	7.72	7.54	1.5	<6	>52
9b	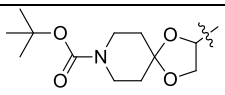	8.12	6.73	>4.8	<6	>5
10b	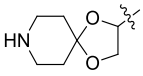	<6	<6	1	<6	1
11b	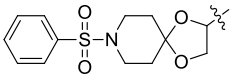	7.28	7.08	1.6	<6	>19
12b	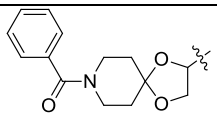	6.90	<6	>8	<6	>8
15b	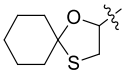	8.90	7.04	72	6.36	346
16b	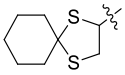	8.21	7.12	12.3	6.78	85

[a] K_i values agreed to ± 20%. [b] Binding assays were performed using 3.0 nM [^{3}H]pentazocine. [c] Binding assays were performed using 3.0 nM [^{3}H]ditolylguanidine. [d] Antilog of the difference between the pK_i values for σ_1 and σ_2 receptors. [e] K_i values were derived from the Cheng–Prusoff equation[43] at one or two concentrations and agreed within 10%. [f] Antilog of the difference between the pK_i values for σ receptors (higher value) and the 5-HT_{1A}R

On the other hand, the benzylated derivatives of **10a** and **10b**, compound **8a** and **8b**, display an increased affinity at σ_1R and σ_2R, although protonation of the same nitrogen atom may occur as well. In particular, compound **8a**, bearing 4-benzylpiperidine moiety highlight a $pK_i\sigma_1$R value (9.08) higher than lead compound **1a** with a similar selectivity ratio (σ_1R/σ_2R = 9). This may be explained by the fact that the introduction of a benzyl moiety increases lipophilicity, which can overcome the negative effect of the positive charge on the nitrogen atom. Adversely, all the amidic and sulphonamidic derivatives coupled with a 4-benzylpiperidine group (**9a**, **11a**, **12a**) or with 1-benzylpiperazine (**9b**, **11b**, **12b**) showed lower affinity values, both at σ_1R and σ_2R. Subsquently, the isosteric substitution of the annular oxygen atoms of the 1,4-dioxa-spiro[4.5]decane moiety of compounds **1a** and **1b** was evaluated. By replacing the oxygen with a sulphur atom at 4-position, to give 1-oxa-4-thiaspiro[4.5]decane derivatives **15a** and **15b**, the affinity at σ_1R and σ_2R are diversely affected. The 1-benzylpiperazine derivative **15b** shows a small decrease in affinity while this decrease is much more marked for the 4-benzylpiperidine **15a**. Replacing both oxygens by sulfur atoms to give 1,4-dithiaspiro[4.5]decane derivatives, again a different behavior was observed for 4-benzylpiperidine **16a** (BS148), and 1-benzylpiperazine **16b** compounds. The latter compounds highlight a further decreased of affinity at σ_1R while the affinity at σ_2R is barely affected. Adversely, for compound **16a** the affinity at the σ_2R remains unchanged whereas at σ_1R it decreases up to 100-fold with respect to compound **1a**, thus giving a reversal of selectivity which shows a value of 0.04.

Therefore, compounds, **1b**, **7b**, **15b**, **16b** and **16a**, were selected for further pharmacological characterization; **1b**, **7b**, **15b**, **16b** for their affinity and selectivity towards σ_1R and **16a** for its affinity and selectivity towards σ_2R.

Molecular modelling studies

The rational design of novel σ_1R ligands is efficiently driven by deepening computational methods, including homology modeling of the biological target[37,42-46,49] as well as pharmacophore-based criteria. Indeed, several series of derivatives fulfilling specific patterns of chemical features have been described in the literature.[49] Most of them were characterized by positive ionizable group and hydrogen bond acceptor functions, connecting at least two hydrophobic cores. Furthermore, docking studies revealed a recurrent binding mode for σ_1R ligands, based on key contacts with an aspartic acid residue (D126), as confirmed by mutagenesis data.[50] More recently, the X-Ray crystallographic structure of the human σ_1R became available, paving the way for the rational design of new compounds (pdb code = 5HK1; resolution = 2.51 Å).[51] In particular, these data allowed the exploration of the binding mode of the co-crystallized ligand PD144418 (1,2,3,6-tetrahydro-5-[3-(4-methylphenyl)-5-isoxazolyl]-1-propylpyridine). As shown in Figure 2, PD144418 exhibited salt bridges between the protonated nitrogen atom of the tetrahydropyridine group and D126 and E172, validating the aforementioned homology models and mutagenesis data. In addition, the ligand was stabilized within the receptor binding site by hydrophobic contacts involving the propyl chain and the phenyl ring and the surrounding amino acids L105, I178 and L182.

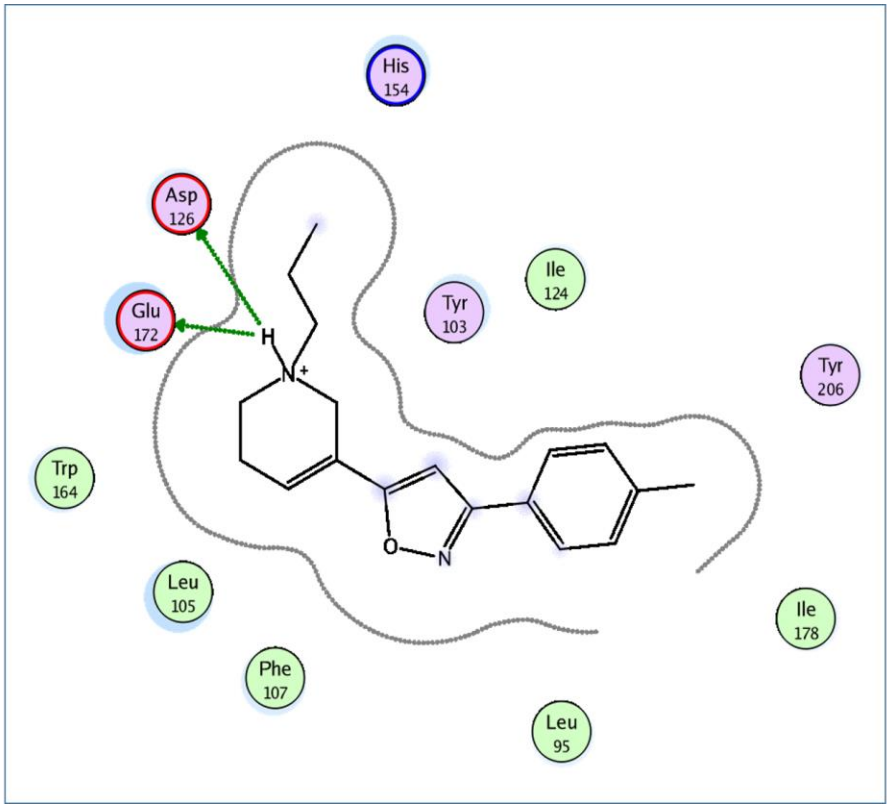

Figure 2. LigPlot of PD144418 co-crystallized with the human σ_1R. Hydrophobic and H-bonding residues are shown in green and in violet, respectively. Negatively- and positively-charged aminoacids are delineated by red and blue lines respectively.

The recently available X-ray crystallographic data of human σ_1, allow to perform more reliable docking calculations. Thus, we had the opportunity to gain more detailed insights into the structure-activity relationship of the newly synthetized compounds through docking studies focused on the σ1 binding site (Table 1S, supporting info). The main issue to be addressed was to clarify the role played by the R portion, in terms of steric and electrostatic properties, when it is coupled with the piperidine or piperazine moiety. An overall perspective of the derived docking poses supports the ability of all compounds to display the required contact with E172, thus being able to anchor the σ_1R. In particular, within the piperidine-series (**a** series) the R substituent and the benzyl moiety were proven to properly mimic the propyl piperidine and the phenyl-oxazole portion of PD144418, respectively

(Figure 3 the docking mode of **1a** is shown, highlighting the *S* enantiomer as the most probable). Indeed, all compounds maintained a common positioning, exhibiting a salt-bridge between the protonated nitrogen atom and E172, while the benzyl moiety occupied a cavity including L105, I178 and L182. On the other hand, the R group was projected towards a receptor deep pocket delineated by F107, Y120, and W164 detecting hydrophobic contacts. Notably, the presence of a small H-bonding heteroatom, such as oxygen for compounds **1a-12a,** allow them to H-bond more efficiently Y120, compared to the corresponding oxathiolane or dithiolane. Bulkier groups proved to be in any case well suited for the piperidine-series, being able to occupy adequately the aforementioned cavity.

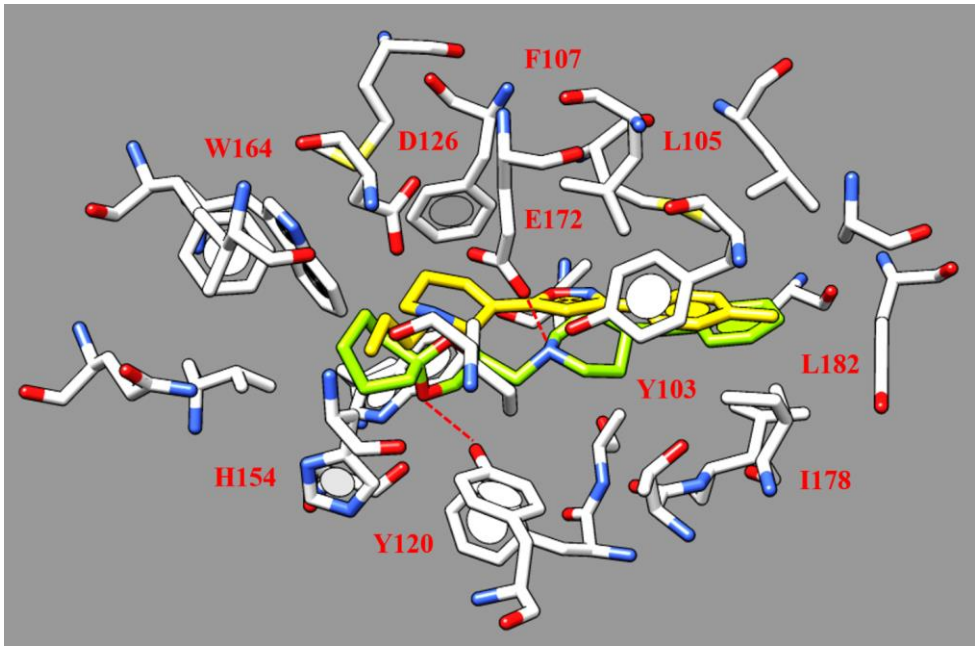

Figure 3. Docking mode of **1a** (*C* atom; green) within the X-ray-derived structure of the human σ_1R co-crystallized with PD144418 (*C* atom; yellow, PDB code 5HK1). The most important residues are labelled. Salt-bridges and H-bonds are illustrated by red, dotted lines.

Conversely, the piperazine-analogues (**b** series) in the presence of small and hydrophobic R groups as for **1b**, **6b**,**15b**, **16b**, exhibited a reversed docking mode, moving the N-benzyl piperazine much more in proximity of the piperidine ring of PD144418, while the R

substituent overlapped the reference phenyl-oxazole, featuring Van der Waals contacts with M93, Y103, I178 and A185. This kind of behavior allowed this series of compounds to better stabilize both the two protonated nitrogen atoms with the E172 side-chain, while no H-bonds involved the R group (Figure 4; docking mode of **1b** is shown being the *R* enantiomer the most probable).

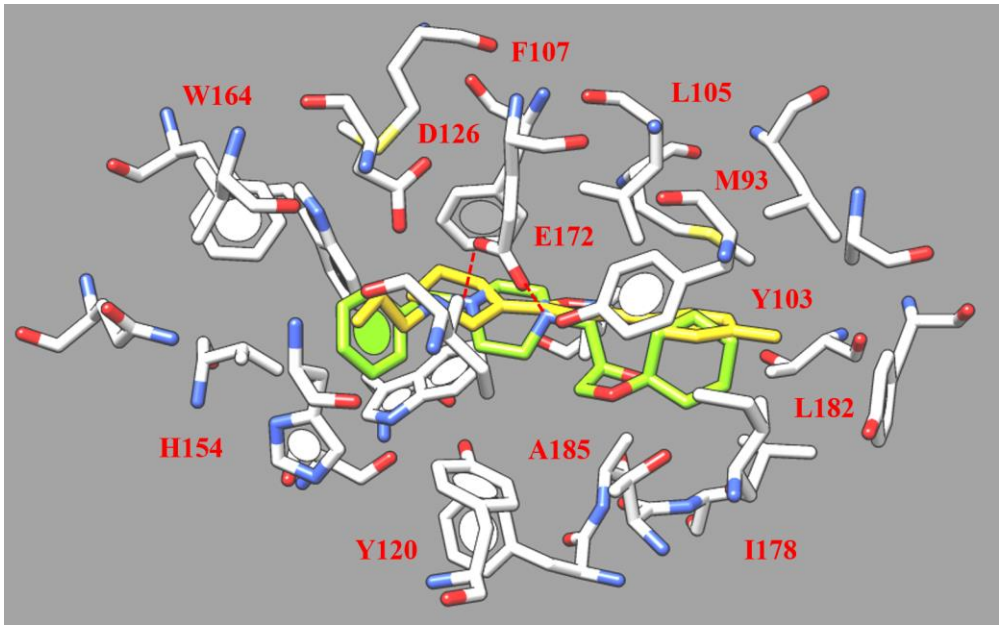

Figure 4. Docking mode of **1b** (*C* atom; green) within the X-ray-derived structure of the human σ_1R co-crystallized with PD144418 (*C* atom; yellow, PDB code 5HK1). The most important residues are labelled. Salt-bridges and H-bonds are shown as red, dotted lines.

Along with this, moving from the dioxolane- to oxathiolane- and dithiolane-, led to piperazines in any case endowed with adequate affinity values for σ_1R, while the binding ability of the related piperidine proved to be deeply impaired, lacking additional H-bonds with Y120. When hindered substituents are placed in R, as for **8b**, **11b**, **12b** ($pK_i\sigma_1$= 6.90-7.72), the piperazines displayed a comparable docking mode with respect to the previously discussed piperidine analogues, therefore detecting only one of the two mentioned salt-bridges, exhibiting lower affinity values than the smaller analogues **1b**, **6b**,**15b**, **16b** ($pK_i\sigma_1$= 8.21-9.13). In conclusion, we can summarize that, with the exception of compounds **7a** and

7b, bulky R groups are required for the piperidine series whilst smaller R are preferred within the piperazine-series.

Analgesic activity

It is known that σ_1R effects the analgesic activity of opioid analgesics, as previously reported .[52] It has been demonstrated that while agonists decrease systemic and supramaximal analgesia, antagonists increase it. Compounds **1b, 7b, 15b, 16a** (BS148) **and 16b,** at the dose of 1.0, 2.0 and 5.0 mg/kg s.c., did not affect basal tail flick latencies (TFLs) during the entire time of observation (data not shown). Injection of MOP agonist morphine, at a dose of 4.0 mg/kg s.c., significantly increased the nociceptive latency following thermal stimulation, which demonstrated a clear analgesic effect (*p<0.05 vs saline treated mice) (Figure 5a). Compared with the group of mice treated with saline, the changes from basal TFL level (Mean Area Under the Curve (MAUC) over 120 min of observation) was increased from 2.69 to 117.3% (Figure 5b).

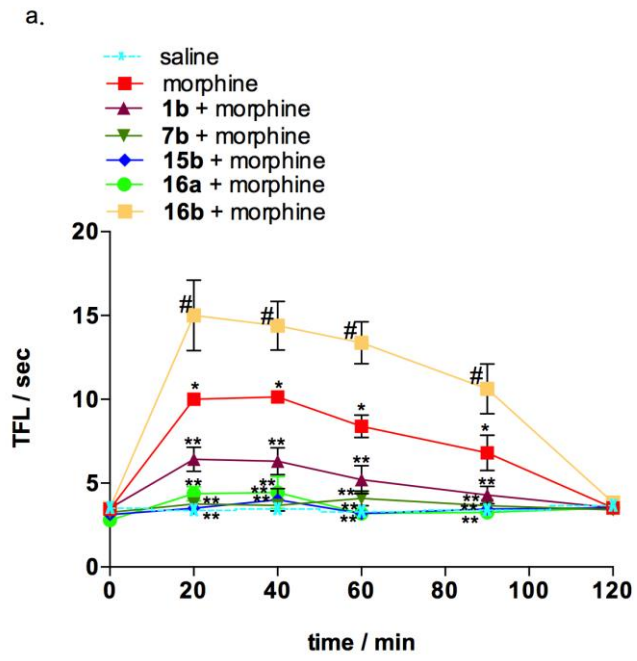

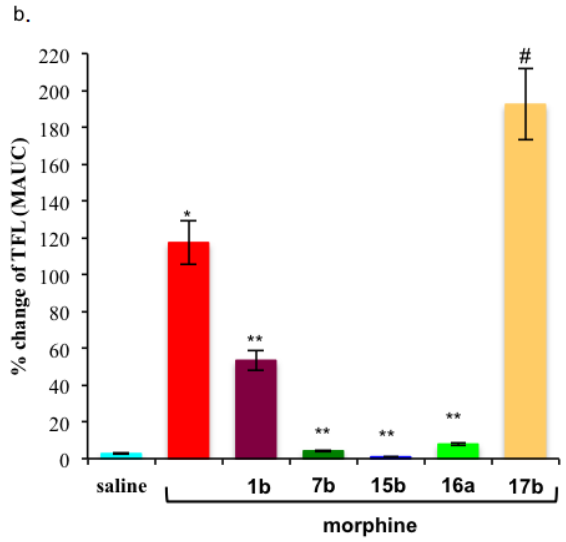

Figure 5. Effects of compounds **1b**, **7b**, **15b**, **16a** (BS148), **16b** (1.0 mg/kg s.c.) on morphine (4 mg/kg s.c.) induced analgesia. Results are expressed in seconds (sec) (**a.**), and as the mean area under the curve (MAUC) (**b.**) after the last injection, over the 120 min testing period. Data are expressed as mean ± SEM from 8-10 mice. *p<0.05 vs saline-treated-mice; **p<0.05 vs morphine-treated-mice; #p<0.05 vs morphine-treated-mice.

Pre-treatment with compounds **1b, 7b, 15b** and **16a**, at 1.0 mg/kg s.c., followed by morphine (4.0 mg/kg s.c.) caused a significant reduction of the opioid analgesic effect. MAUC value was significantly lower than that in mice treated with opioid alone: 53.3, 4.1, 0.95 and 7.85 vs 117.3 respectively for compounds **1b, 7b, 15b** and **16a**, (**p<0.01 vs morphine treated mice) (Figure 5b). The decrease of the analgesic effect was seen for the entire period of observation. These results are consistent with an agonistic behavior of these compounds at σ_1 receptors, confirming results previously reported with **1b** on a rat preparation.[39] In contrast, pre-treatment with **16b** at 1.0 mg/kg s.c., followed by morphine injection (4.0 mg/kg s.c.) caused an increase in the opioid analgesic effect and the MAUC value was significantly higher than that of mice receiving morphine alone (192.4% with respect to 117.3%) (#p<0.05 vs morphine treated mice) (Figure 5b), suggesting an antagonist profile at σ_1R. This results is

of certain interest as the enhancement of the analgesic effect could reduce the dose of opioid agonists in pain therapy, minimizing the adverse effects of opiate treatments.[53] Furthermore, it has been shown that σ_1R antagonists may have promising antinociceptive properties in different neurogenic pain models.[54] It has also been shown that high affinity and selective σ_1R antagonists dose-dependently inhibited mechanical allodynia which was reversed completely by the application of selective σ_1R agonist.[55] Therefore, compound **16b** deserves further investigation.

Anti-proliferative activity

In the current study, the effect on cell viability of compounds **1b**, **7b**, **10a**, **15b**, **16a** (BS148) and **16b** was primarily tested on two melanoma cell lines: SK-MEL-28, derived from primary melanoma and SK-MEL-2, derived from metastatic melanoma.[56,57] Siramesine, a potent σ_2R agonist and a proven potent cell toxicity inducer, was used as a positive control for cell death.[58,59] In vitro toxicity of the compounds was determined by MTT cell viability assay. Each experiment was performed in triplicate, in three independent experiments, at a concentration of 20, 40, 80 and 100μM, in order to obtain dose dependent curves.

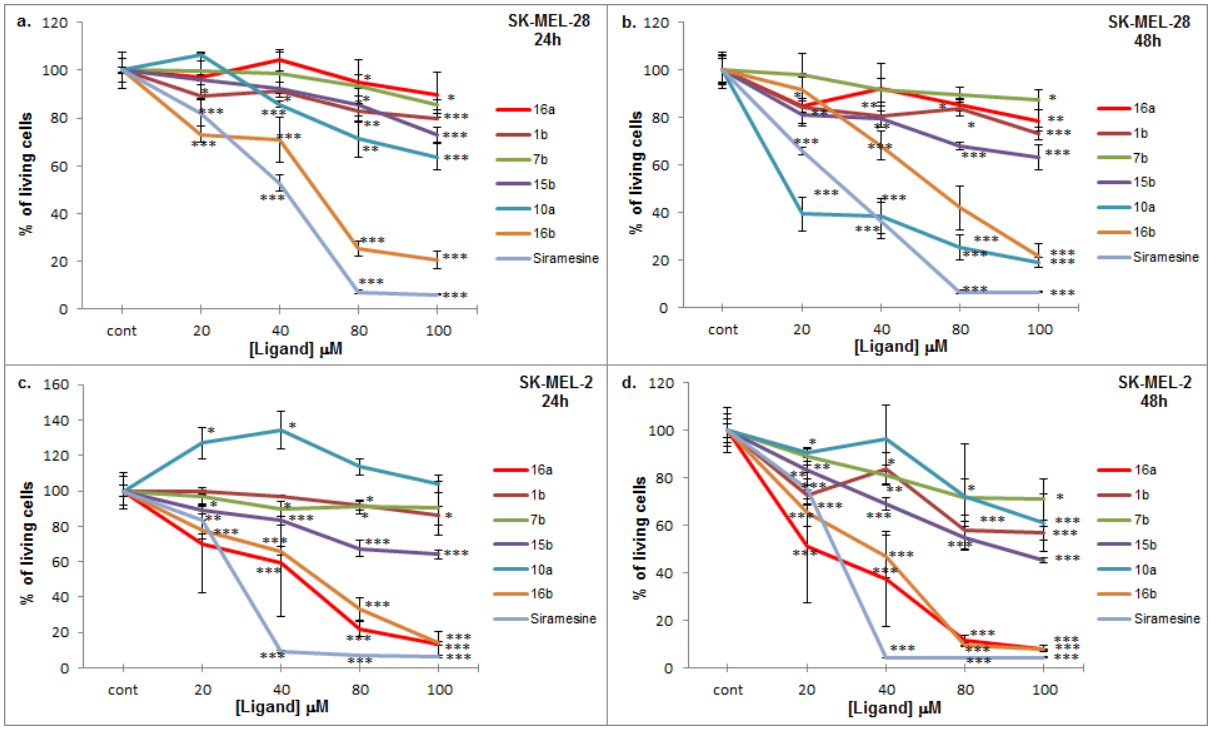

Figure 6. Dose-response curves of compounds **1b**, **7b**, **10a**, **15b**, **16a** (BS148), **16b** and Siramesine in MTT cell viability assay on SK-MEL-28 (a, b) or SK-MEL-2 (c, d) cell lines. Cells were treated with increasing concentrations (from 20 to 100µM) of tested compounds and monitored at 24 (a, c) and 48 hours (b, d). Data are expressed as mean ± SEM for the three independent experiments, each performed in triplicate. *p<0.05 vs untreated-cells; **p<0.01 vs untreated-cells; ***p<0.001 vs untreated-cells.

As shown in Figure 6, almost all tested compounds decreased cell viability in varying percentages. In the primary melanoma model (SK-MEL-28), with the exception of **10a** and **16b** (at a concentration higher than 40µM**)**, cell survival at 48h was more than 50% when compared to the untreated control. However, Siramesine confirmed its toxic profile, showing only 8% cell survival at 80µM. In the metastatic melanoma model (SK-MEL-2) the **16a** (BS148) and **16b** were the only compounds able to decrease cell viability under 50%, both at 24 and 48 hours, with a IC_{50} of 52µM and 22µM for **16a** and 50µM and 38µM for **16b**, respectively. Siramesine again confirmed its toxic profile, with cell survival of only 5% at

40µM. Interestingly, in this experimental model **10a**, especially at low concentrations (20-40 µM), exhibited a hyper proliferation behavior, increasing cell viability by 30% at 24h ($p<0.05$ vs untreated-cells).

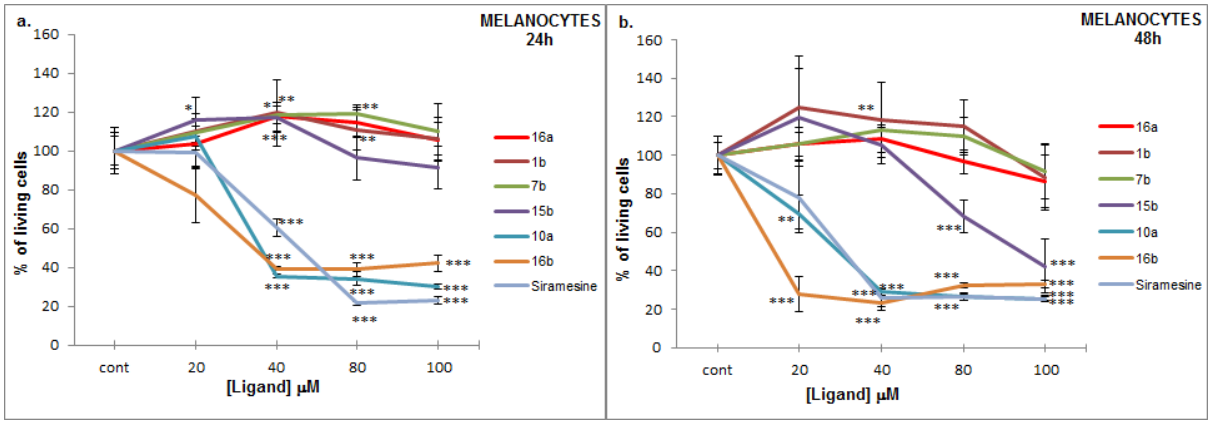

Figure 7. Dose-response curves of compounds **1b**, **7b**, **10a**, **15b**, **16a** (BS148), **16b** and Siramesine in MTT cell viability assay on normal human melanocytes. Cells were treated with increasing concentrations (from 20 to 100µM) of tested compounds and monitored at 24 (a) and 48 hours (b). Data are expressed as mean ± SEM from three independent experiments, each performed in triplicate. *$p<0.05$ vs untreated-cells; **$p<0.01$ vs untreated-cells; ***$p<0.001$ vs untreated-cells.

Effect on cell viability of compounds **1b**, **7b**, **10a**, **15b**, **16a** (BS148) and **16b** were also tested on healthy melanocytes to check any toxic potential. Again, Siramesine was employed as a control compound for cell death. As shown in Figure 7, Siramesine exhibited the expected cell toxicity in a dose dependent manner. Toxicities of compounds **10a** and **16b** were similar to Siramesine, both at 24 and 48 hours. Compounds **1b**, **7b**, **16a** (BS148) and **15b** did not show any toxic effect at 24h and only **15b** decreased cells viability under 50% at 48h and only at extremely high concentrations (80-100 µM). According to these results BS148, showed a remarkable selective toxicity for SK-MEL-2 and seems to be a promising compound for metastatic melanoma therapy.

The results of this study provide additional information about both the sigma pharmacology of these molecules and the employed melanoma cancer models. Based on the results of the binding experiments (Tables 1 and 2) BS148 was found to be the only compound to show a marked σ_2R selectivity. According to MTT assay, the selective toxicity of BS148, revealed a σ_2 agonist profile, which is consistent with current literature indicating that σ_2R activation is responsible for cell death.[36] The in-vivo analgesia studies demonstrated that BS148 behaves as a σ_1R agonist thus excluding the involvement of σ_1R in cell death, as it is already known that only antagonist at σ_1R affects cell proliferation.[37] Furthermore, the selective death of metastatic SK-MEL-2 cells caused by BS148 may also unveil different σR expression patterns, suggesting that the σ_2R subtype could be over expressed in metastatic melanoma cells. Regardless of the exact mechanism of action, the lack of toxicity on healthy melanocytes suggests that BS148 is a promising candidate to be developed as a novel drug in melanoma chemotherapy. In an initial attempt to understand, whenever possible, the mechanism of action of BS148, DNA fragmentation was measured by terminal deoxynucleotidyl transfer-mediated dUTP nick-end labeling (TUNEL) for the detection of apoptotic cells. Normal human melanocytes, SK-MEL-2 and SK-MEL-28 cell lines were treated with BS148 at a dose of 20 and 40μM at 24 (data not shown) and 48 hours. Both negative controls (untreated cells) and positive controls (Siramesine 40μM, 98% of apoptotic cells, data not shown) were employed.

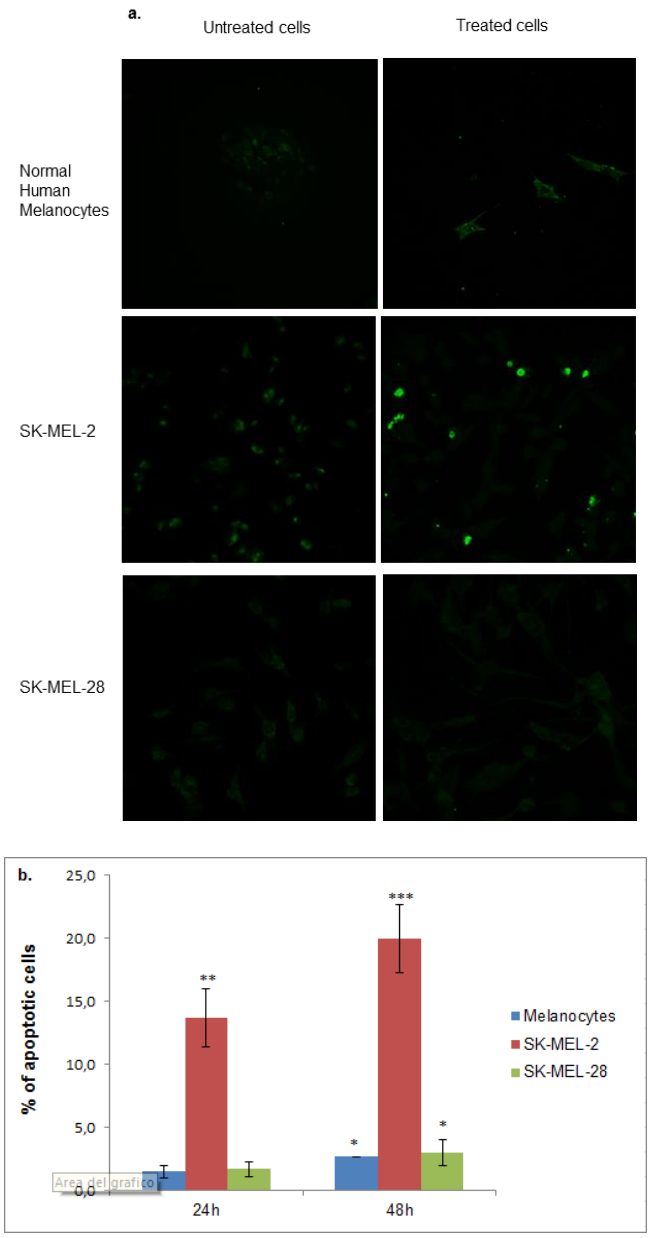

Figure 8. TUNEL assay. a) Fluorescence microscopy images of normal human melanocytes, SK-MEL-2 and SK-MEL-28 cell lines after treatment with **16a** (BS148) 40 µM (right column) at 48 hours. Untreated cells were used as a negative control (left column). Green cells are positive for DNA fragmentation. b) Percentage of positive cells after **16a** treatment (40 µM) on normal human melanocytes, SK-MEL-2 and SK-MEL-28 cell lines at 24 and 48 hours. Error bars represent the standard deviation of triplicate independent experiments performed in triplicate. *p<0.05 vs untreated-cells; **p<0.01 vs untreated-cells; ***p<0.001 vs untreated-cells.

More than 20% of positive cells were detected by fluorescence microscopy in SK-MEL-2 treated samples (**16a**, 40 µM) at 48 hours while almost no apoptotic cells (<3%) were present in normal human melanocytes and SK-MEL-28 cell lines (Figure 8a). The number of apoptotic cells proportionally increases with longer time of exposure (from 24 to 48 hours) (Figure 8b). These preliminary results suggest that the apoptotic pathway is involved in σ_2R induced cell death, but apoptosis is only partly responsible for cell death. Recently, other authors have shown that σ_2R ligands induce tumor cell death in human melanoma cell lines MDA-MB-435 by multiple signaling pathways, such as autophagy and deregulation of cell-cycle.[36] However, more research is needed to better define the functional activity of BS148 and future investigations into cell death mechanisms should focus on oxidative stress induction. Further research should also consider recent findings on tumor cell lines, which strongly suggest the loss of mitochondrial integrity as a critical factor for cell death induction.[58]

Conclusion

Starting from the 1,4-dioxa-spiro[4.5]decane derivatives **1a** and **1b**, eighteen new compounds were synthetized and studied. Most were found to have affinity for σ_1R in the nanomolar range. The most interesting compounds were further studied to determine a functional behavior. In the tail-flick test **7b, 15b** and **16a** (BS148) decreased the analgesic effect of morphine which allowed to define them as σ_1R agonists. Conversely, **16b** was able to potentiate this effect defining it as σ_1R antagonist. In the anti-proliferative study, BS148, the only one to exhibit σ_2R selectivity, was able to induce a selective toxicity towards SK-MEL-2, a metastatic malignant melanoma cell line, whilst not affecting normal human melanocytes. These results suggest an agonistic profile at σ_2R. Malignant melanoma cell death induced by BS148 was at least in part due to apoptosis, as indicated by Tunnel assay.

The current study suggests that BS148 should be further investigated as a promising candidate for novel metastatic melanoma therapy development.

Experimental Section

Chemistry

General methods

All reagents, solvents and other chemicals were used as purchased from Sigma-Aldrich without further purification unless otherwise specified. Air- or moisture-sensitive reactants and solvents were employed in reactions carried out under nitrogen atmosphere unless otherwise noted. Microwave assisted synthesis was conducted by using a CEM Discover Labmate (CEM Corp., Matthews, NC). Flash column chromatography purifications (medium pressure liquid chromatography) were carried out using Merck silica gel 60 (230-400 mesh, ASTM). The purity of compounds was determined by elemental analysis (C,H,N) that was performed on a Carlo Erba 1106 Analyzer in the Microanalysis Laboratory of the Life Sciences Department of Università degli Studi di Modena e Reggio Emilia and the results here reported are within ±0.4% of the theoretical values. Melting points were determined with a Stuart SMP3 and they are uncorrected. The structures of all isolated compounds were ensured by Nuclear magnetic resonance (NMR) and Mass spectrometry. ^{1}H and ^{13}C NMR (1D and 2D experiments) spectra were recorded on a DPX-200 Advance (Bruker) spectrometer operating at 200.13 MHz and on a DPX-400 Advance (Bruker) spectrometer operating at 400.13 MHz Chemical shifts are expressed in δ (ppm). ^{1}H NMR chemical shifts are relative to tetramethylsilane (TMS) as internal standard. ^{13}C NMR chemical shifts are relative to TMS at δ 0.0 or to the ^{13}C signal of the solvent: $CDCl_3$ δ 77.04, CD_3OD δ 49.8, DMSO-d_6 δ 39.5. NMR data are reported as follows: chemical shift, number of protons/carbons, multiplicity (s, singlet; d, doublet; t, triplet; q, quartet; m, multiplet; br,

broadened), coupling constants (Hz) and assignment (Dotsd= 1,4-dioxa-8-thiaspiro[4.5]decane; Tosd= 1,4,8-trioxaspiro[4.5]decane; Doasd= 1,4-dioxa-8-azaspiro[4.5]decane; Bz= benzyl; Piper..= piperidine or piperazine; Phe= phenyl; Bz= benzoyl; Ts= tosyl;). ^{1}H-^{1}H correlation spectroscopy (COSY), ^{1}H-^{13}C heteronuclear single quantum coherence (HSQC) and heteronuclear multiple bond connectivity (HMBC) experiments were recorded for determination of ^{1}H-^{1}H and ^{1}H-^{13}C correlations respectively. HR-MS experiments were carried out using a LC-MS mass spectrometer (6520 Accurate-Mass Q-TOF LC/MS - Agilent Technologies) equipped with an ion spray ionization source (ESI). MS (+) spectra were acquired by direct infusion (5 ml/min) of a solution containing the appropriate sample as oxalate salt (100 pmol/ml), dissolved in a 0.1% acetic acid solution, with mobile phase methanol/water 50:50, at the optimum ion voltage of 4800 V. The yields reported are based on a single experiment and are not optimized. The oxalate salts of all tested compounds were used for the pharmacological evaluations. All tested compounds possess a purity of at least 95% as determined by combustion analysis.

General procedure A

To a solution of 4-benzylpiperidine or 1-benzylpiperazine (3.0 mmol), KI (0.2 mmol) in anhydrous 2-methoxyethanol (10 mL) was added the selected halogen derivative **2-5**[42] and **13**, **14**[43] (1.0 mmol) portion wise. The resulting mixture was heatedto reflux for 12 h or using microwave irradiation (160°C for 30 min) then cooled to room temperature and concentrated *in vacuum*. The residue was partitioned between EtOAc and H_2O. The organic layer was separated, and the aqueous layer was extracted with EtOAc. The organic layers were combined, washed with H_2O, dried over anhydrous Na_2SO_4, filtered, and concentrated *in vacuum*. The residue was purified by flash chromatography to yield the desired compound.

1-(1,4-Dioxa-8-thiaspiro[4.5]decan-2-ylmethyl)-4-benzylpiperidine (6a)

The title compound was obtained as a yellow oil from **2** and 4-benzylpiperidine following the general procedure A (0.171 g, 0.49 mmol, yield 70%). The free amine (0.15 g, 0.4 mmol) was then converted into the corresponding hydrogenoxalate from diethyl ether (0.134 g, 0.306 mmol, yield 70%); mp: 188-190°C; HRMS-ESI: *m/z* $[M+H]^+$ calcd for $C_{20}H_{30}NO_2S$: 348.1992, found: 348.1993; Anal. calcd for $C_{22}H_{31}NO_6S$: C 60.39, H 7.14, N 3.20, found: C 60.58, H 7.34, N 3.31.

1-(1,4-Dioxa-8-thiaspiro[4.5]decan-2-ylmethyl)-4-benzylpiperazine (6b)

The title compound was obtained as an oil from **2** and 1-benzylpiperazine following the general procedure A (0.353 g, 1.01 mmol, yield 85%). The free amine (0.15 g, 0.43 mmol) was then converted into the corresponding hydrogenoxalate from diethyl ether (0.194 g, 0.37 mmol, yield 85%); mp: 217-219°C; HRMS-ESI: *m/z* $[M+H]^+$ calcd for $C_{19}H_{29}N_2O_2S$: 349.1944, found: 349.1945; Anal. calcd for $C_{23}H_{32}N_2O_{10}S$: C 52.26, H 6.10, N 5.30, found: C 52.33, H 6.05, N 5.43.

1-(1,4,8-Trioxaspiro[4.5]decan-2-ylmethyl)-4-benzylpiperidine (7a)

The title compound was obtained as a yellow oil from **3** and 4-benzylpiperidine following the general procedure A (0.37 g, 1.11 mmol, yield 86%). The free amine (0.15 g, 0.45 mmol) was then converted into the corresponding hydrogenoxalate from diethyl ether (0.04 g, 0.093 mmol, yield 27%); mp: 177-179°C; HRMS-ESI: *m/z* $[M+H]^+$ calcd for $C_{20}H_{30}NO_3$: 332.2220, found: 332.2222; Anal. calcd for $C_{22}H_{31}NO_7$: C 62.69, H 7.41, N 3.32, found: C 62.92, H 7.67, N, 3.56.

1-(1,4,8-Trioxaspiro[4.5]decan-2-ylmethyl)-4-benzylpiperazine (7b)

The title compound was obtained as an oil from **3** and 1-benzylpiperazine following the general procedure A (0.129 g, 0.387 mmol, yield 58%). The free amine (0.12 g, 0.36 mmol) was then converted into the corresponding hydrogenoxalate from diethyl ether (0.084 g, 0.164 mmol, yield 45%); mp: 226-227°C; HRMS-ESI: *m/z* $[M+H]^+$ calcd for $C_{19}H_{29}N_2O_3$: 333.2173, found: 333.2174; Anal. calcd for $C_{23}H_{32}N_2O_{11}$: C 53.90, H 6.29, N 5.74, found: C 54.11, H 6.47, N 5.90.

8-Benzyl-2-((4-benzylpiperidin-1-yl)methyl)-1,4-dioxa-8-azaspiro[4.5]decane (8a)

The title compound was obtained as a yellow oil from **4** and 4-benzylpiperidine following the general procedure A (1.23 g, 2.94 mmol, yield 82%). The free amine (0.15 g, 0.35 mmol) was then converted into the corresponding hydrogenoxalate from diethyl ether (0.064 g, 0.104 mmol, yield 35%); mp: 75-77°C; HRMS-ESI: *m/z* $[M+H]^+$ calcd for $C_{27}H_{37}N_2O_2$: 421.2850, found: 421.2851; Anal. calcd for $C_{31}H_{40}N_2O_{10}$: C 61.99, H 6.71, N 4.66, found: C 62.24, H 6.83, N 4.87.

8-benzyl-2-((4-benzylpiperazin-1-yl)methyl)-1,4-dioxa-8-azaspiro[4.5]decane (8b)

The title compound was obtained as an oil from **4** and 1-benzylpiperazine following the general procedure A (1.3 g, 3.1 mmol, yield 77%). The free amine (0.15 g, 0.36 mmol) was then converted into the corresponding hydrogenoxalate from diethyl ether (0.148 g, 0.214 mmol, yield 60%); mp: 148-150°C; HRMS-ESI: *m/z* $[M+H]^+$ calcd for $C_{26}H_{36}N_3O_2$: 422.2802, found: 422.2804; Anal. calcd for $C_{32}H_{41}N_3O_{14}$: C 55.57, H 5.97, N 6.08, found: C 55.61, H 6.15, N 6.23.

***Tert*-butyl 2-((4-benzylpiperidin-1-yl)methyl)-1,4-dioxa-8-azaspiro[4.5]decane-8-carboxylate (9a)**

The title compound was obtained as a yellow oil from **5** and 4-benzylpiperidine following the general procedure A (0.56 g, 1.3 mmol, yield 40%). The free amine (0.25 g, 0.58 mmol) was then converted into the corresponding hydrogenoxalate from diethyl ether (0.168 g, 0.32 mmol, yield 56%); mp: 98-100°C; HRMS-ESI: *m/z* $[M+H]^+$ calcd for $C_{25}H_{38}N_2O_4$: 431.2905, found: 431.2922; Anal. calcd for $C_{27}H_{40}N_2O_8$: C 62.69, H 7.74, N 5.38, found: C 62.88, H 7.88, N 5.45.

***Tert*-butyl 2-((4-benzylpiperazin-1-yl)methyl)-1,4-dioxa-8-azaspiro[4.5]decane-8-carboxylate (9b)**

The title compound was obtained as an oil from **5** and 1-benzylpiperazine following the general procedure A (0.04 g, 0.093 mmol, yield 27%). The free amine (0.04 g, 0.093 mmol) was then converted into the corresponding hydrogenoxalate from diethyl ether (0.060 g, 0.093 mmol, yield 99%); mp: 216-218°C; HRMS-ESI: *m/z* $[M+H]^+$ calcd for $C_{24}H_{38}N_3O_4$: 432.2852, found: 432.2863; Anal. calcd for $C_{28}H_{41}N_3O_{12}$: C 54.98, H 6.76, N 6.87, found: C 55.13, H 6.91, N 7.01.

General Procedure B

To a stirred solution of **9a** or **9b** (0.035 g, 0.081 mmol) in CH_2Cl_2 (2 mL), trifluoroacetic acid (2.6 mmol, 0.2 mL) was added. The resulting mixture was stirred at room temperature for 3 h, subsequently the organic phase was washed with a solution of NaOH 5%, dried over anhydrous Na_2SO_4. The suspension obtained was filtered, then the solution was concentrated under vacuum to give the desired compound.

2-((4-benzylpiperidin-1-yl)methyl)-1,4-dioxa-8-azaspiro[4.5]decane (10a)

The title compound was obtained as a yellow oil from **9a** following the general procedure B (0.025 g, 0.076 mmol, 93% yield). The free amine (0.125 g, 0.379 mmol) was then converted into the corresponding hydrogenoxalate from diethyl ether (0.148 g, 0.29 mmol, yield 77%); mp: 155-157°C; HRMS-ESI: *m/z* $[M+H]^+$ calcd for $C_{24}H_{38}N_3O_4$: 331.2380, found: 331.2393; Anal. calcd for $C_{24}H_{34}N_2O_{10}$: C 56.46, H 6.71, N 5.49, found: C 56.63, H 6.95, N 5.39.

2-((4-benzylpiperazin-1-yl)methyl)-1,4-dioxa-8-azaspiro[4.5]decane (10b)

The title compound was obtained as a yellow oil from **9b** following the general procedure B (0.012 g, 0.036 mmol, 43% yield). The free amine (0.198 g, 0.600 mmol) was then converted into the corresponding hydrogenoxalate from diethyl ether (0.265 g, 0.44 mmol, yield 74%); mp: 231-232°C; HRMS-ESI: *m/z* $[M+H]^+$ calcd for $C_{19}H_{30}N_3O_2$: 332.2330, found: 332.2343; Anal. calcd for $C_{25}H_{35}N_3O_{14}$: C 49.92, H 5.86, N 6.99, found: C 50.12, H 5.98, N 7.21.

General Procedure C

The selected benzenesulfonyl chloride and/or benzoyl chloride(1.2 mmol) was added at 0°C to a solution of compound **10a** or **10b** (1 mmol) and triethylamine (2 mmol) in dry CH_2Cl_2 (5 mL). The mixture was stirred at room temperature for 12 h. Ice and water were then added and extractions were made with CH_2Cl_2. The organic layers were combined and dried over anhydrous Na_2SO_4. The suspension obtained was filtered and the solution was concentrated under vacuum to give a solid residue which was purified by column chromatography providing the expected compound.

2-((4-Benzylpiperidin-1-yl)methyl)-8-(phenylsulfonyl)-1,4-dioxa-8-azaspiro[4.5]decane(11a)

The title compound was obtained as an oil from **10a** and benzensulfonylchloride following the general procedure C (0.09 g, 0.19 mmol, yield 32%). The free amine (0.084 g, 0.18 mmol) was then converted into the corresponding hydrogenoxalate from diethyl ether (0.030 g, 0.054 mmol, yield 30%); mp: 155-156°C; HRMS-ESI: *m/z* $[M+H]^+$ calcd for $C_{26}H_{35}N_2O_4S$: 471.2312, found: 471.2326; Anal. calcd for $C_{28}H_{36}N_2O_8S$: C 59.98, H 6.47, N 5.00, found: C 60.22, H 6.65, N 5.27.

2-((4-benzylpiperazin-1-yl)methyl)-8-(phenylsulfonyl)-1,4-dioxa-8-azaspiro[4.5]decane (11b)

The title compound was obtained as an oil from **10b** and benzensulfonyl chloride following the general procedure C (0.184 g, 0.392 mmol, yield 67%). The free amine (0.057 g, 0.121 mmol) was then converted into the corresponding hydrogenoxalate from diethyl ether (0.047 g, 0.072 mmol, yield 60%); mp: 214-216°C; HRMS-ESI: *m/z* $[M+H]^+$ calcd for $C_{25}H_{34}N_3O_4S$: 472.2265, found: 472.2276; Anal. calcd for $C_{29}H_{37}N_3O_{12}S$: C 53.45, H 5.72, N 6.45, found: C 53.68, H 5.93, N 6.71.

(2-((4-benzylpiperidin-1-yl)methyl)-1,4-dioxa-8-azaspiro[4.5]decan-8-yl)(phenyl)methanone (12a)

The title compound was obtained as an oil from **10a** and benzoyl chloride following the general procedure C (0.119 g, 0.274 mmol, yield 57%). The free amine (0.119 g, 0.27 mmol) was then converted into the corresponding hydrogenoxalate from diethyl ether (0.101 g, 0.192 mmol, yield 71%); mp: 128-130°C; HRMS-ESI: *m/z* $[M+H]^+$ calcd for $C_{27}H_{35}N_2O_3$: 435.2642, found: 435.2654; Anal. calcd for $C_{29}H_{36}N_2O_7$: C 66.39, H 6.92, N 5.34, found: C 66.63, H 7.02, N 5.56.

(2-((4-benzylpiperazin-1-yl)methyl)-1,4-dioxa-8-azaspiro[4.5]decan-8-yl)(phenyl)methanone (12b)

The title compound was obtained as an oil from **10b** and benzoyl chloride following the general procedure C (0.264 g, 0.60 mmol, yield 73%). The free amine (0.139 g, 0.32 mmol) was then converted into the corresponding hydrogenoxalate from diethyl ether (0.20 g, 0.325 mmol, yield 99%); mp: 216-218°C; HRMS-ESI: *m/z* $[M+H]^+$ calcd for $C_{26}H_{34}N_3O_3$: 436.2595, found: 436.6020; Anal. calcd for $C_{30}H_{37}N_3O_{11}$: C 58.53, H 6.06, N 6.83, found: C 58.84, H 6.21, N 6.94.

1-(1-oxa-4-thiaspiro[4.5]decan-2-ylmethyl)-4-benzylpiperidine (15a)

The title compound was obtained as a yellow oil from **13**[43] and 4-benzylpiperidine following the general procedure A (0.162 g, 0.471 mmol, yield 65%). The free amine (0.15 g, 0.43 mmol) was then converted into the corresponding hydrogenoxalate from diethyl ether (0.130g, 0.30 mmol, yield 70%); mp: 172-173°C; HRMS-ESI: *m/z* $[M+H]^+$ calcd for $C_{21}H_{32}NOS$: 346.2199, found: 346.2207; Anal. calcd for $C_{23}H_{33}NO_5S$: C 63.42, H 7.64, N 3.22, found: C 63.57, H 7.81, N 3.46.

1-(1-oxa-4-thiaspiro[4.5]decan-2-ylmethyl)-4-benzylpiperazine (15b)

The title compound was obtained as an oil from **13**[43] and 1-benzylpiperazine following the general procedure A (0.20 g, 0.578 mmol, yield 79%). The free amine (0.20 g, 0.578 mmol) was then converted into the corresponding hydrogenoxalate from diethyl ether (0.223 g, 0.424 mmol, yield 73%); mp: 236-238°C; HRMS-ESI: *m/z* $[M+H]^+$ calcd for $C_{20}H_{31}N_2OS$: 347.2152, found: 347.2164; Anal. calcd for $C_{24}H_{34}N_2O_9S$: C 54.74, H 6.51, N 5.32, found: C 54.89, H 6.74, N 5.39.

1-(1,4-dithiaspiro[4.5]decan-2-ylmethyl)-4-benzylpiperidine (16a)

The title compound was obtained as a yellow oil from **14**[43] and 4-benzylpiperidine following the general procedure A (0.07 g, 0.191 mmol, yield 28%). The free amine (0.07 g, 0.191 mmol) was then converted into the corresponding hydrogenoxalate from diethyl ether (0.086 g, 0.190 mmol, yield 99%); mp: 132-134°C; HRMS-ESI: *m/z* $[M+H]^+$ calcd for $C_{21}H_{32}NS_2$: 362.1971, found: 362.1978; Anal. calcd for $C_{23}H_{33}NO_4S_2$: C 61.16, H 7.36, N 3.10, found: C 60.97, H 7.22, N 3.01.

1-(1,4-dithiaspiro[4.5]decan-2-ylmethyl)-4-benzylpiperazine (16b)

The title compound was obtained as an oil from **14**[43] and 1-benzylpiperazine following the general procedure A (0.168 g, 0.464 mmol, yield 69%). The free amine (0.094 g, 0.26 mmol) was then converted into the corresponding hydrogenoxalate from diethyl ether (0.09 g, 0.167 mmol, yield 64%); mp: 230-231°C; HRMS-ESI: *m/z* $[M+H]^+$ calcd for $C_{20}H_{30}N_2S_2$: 363.1923, found: 363.1916; Anal. calcd for $C_{24}H_{34}N_2O_8S_2$: C 53.12, H 6.32, N 5.16, found: C 53.38, H 6.51, N 5.38.

Biology

Radioligand Binding Assay at σR

In vitro σ-binding experiments were carried out as previously reported.[60] $\sigma_1$binding assays were performed on guinea pig brain membranes according to experimental protocol described by De Haven et al.[61] Briefly, 500 μg of membrane protein was incubated with 3 nM [^{3}H]-(+)-pentazocine (29 C_i/mM; the value of the apparent dissociation constant (K_d) was 14 ± 0.3 nM, n= 3) in 50 mM Tris-HCl (pH 7.4). Test compounds were added in concentration ranging from 10^{-5} to 10^{-11} M. Nonspecific binding was assessed in the presence of 10 μM of unlabeled haloperidol. The reaction was performed for 150 min at 37°C and terminated by

filtering the solution through Whatman GF/B glass fiber filters which were presoaked for 1 h in a 0.5% poly(ethyleneimine) solution. Filters were washed with ice cold buffer (2 × 4 mL). Regarding σ_2-binding assays,[62] the membranes were incubated with 3 nM [^{3}H]DTG (53.3 C_i/mM; K_d = 11 ± 0.8 nM; n = 3) in the presence of 400 nM (+)-SKF10,047 so as to mask σ_1 sites. Nonspecific binding was evaluated with DTG (5 μM). Incubation was carried out in 50 mM Tris-HCl (pH 8.0) for 120 min at room temperature, and assays were terminated by the addition of ice-cold 10 mM Tris-HCl (pH 8.0). Each sample was filtered through Whatman GF/B glass fibers filters, which were presoaked for 1 h in a 0.5% poly(ethylenimine) solution, using a Millipore filter apparatus. Filters were washed twice with 4 mL of ice-cold buffer. Radioactivity was counted in 4 mL of "Ultima Gold MV" in a 1414 Winspectral PerkinElmer Wallac liquid scintillation counter. Inhibition constants (K_i values) were calculated using the EBDA/LIGAND program purchased from Elsevier/Biosoft.

Radioligand Binding Assay at Human Recombinant 5-HT_{1A}R

A human cell line (HeLa) stably transfected with genomic clone G-21 coding for the human 5-HT_{1A} serotoninergic receptor was used. The cells were grown as monolayers in Dulbecco's modified Eagle's medium supplemented with 10% fetal calf serum and gentamycin (100 μg/mL) under 5% CO_2 at 37°C. The cells were detached from the growth flask at 95% confluence by a cell scraper and were lysed in ice-cold Tris (5 mM) and EDTA buffer (5 mM, pH 7.4). The homogenates were centrifuged for 20 min at 40000g, and the pellets were re-suspended in a small volume of ice-cold Tris/EDTA buffer (above) and immediately frozen and stored at 70°C until use. On the day of experiment, cell membranes (80-90 μg of protein) were re-suspended in binding buffer (50 mM Tris, 2.5 mM $MgCl_2$, and 10 mM Pargiline, pH 7.4). The membranes were incubated in a final volume of 0.32 mL for 30 min at 30 °C with 1 nM [^{3}H]8-OH-DPAT, in the absence or presence of various concentrations of

the competing drugs (1pM to 1 μM); each experimental condition was performed in triplicate. Nonspecific binding was determined in the presence of 10 μM 5-HT.[63]

Molecular Modelling

All the compounds were built, parameterized (Gasteiger-Huckel method) and energy minimized within MOE using MMFF94 forcefield [MOE: Chemical Computing Group Inc . Montreal. H3A 2R7 Canada. http://www.chemcomp.com]. For the newly synthesized compounds, the two *R* and *S* enantiomers were taken into account and built *in silico*.

Docking calculations within the X-ray structure of human sigma-1 receptor (pdb code = 5HK1) were performed using the Surflex docking module implemented in Sybyl-X1.0 [Sybyl-X 1.0 Tripos Inc 1699 South Hanley Road. St Louis. Missouri. 63144. USA 25] Surflex-Dock uses an empirically derived scoring function based on the binding affinities of X-ray protein-ligand complexes. The Surflex-Dock scoring function is a weighted sum of non-linear functions involving van der Waals surface distances between the appropriate pairs of exposed protein and ligand atoms, including hydrophobic, polar, repulsive, entropic and solvation and crash terms represented in terms of a total score conferred to any calculated conformer. Then, the best docking geometry (selected on the basis of the SurFlex scoring functions) was refined by ligand/protein complex energy minimization (CHARMM27) by means of the MOE software. Finally, the protein-ligand complex stability was successfully assessed using a short ~1 ps run of molecular dynamics (MD) at constant temperature, followed by an all-atom energy minimization (LowModeMD implemented in MOE software). This kind of module allowed to perform an exhaustive conformational analysis of the ligand-receptor binding site complex, as we already discussed about other case studies, where it proved to be useful for a preliminary evaluation of docking poses.[42, 64, 65]

In vivo biological assay

Animals

Male CD1 mice (Harlan, Italy), weighing 25-30 g, were used.

Animals were kept at a constant room temperature (25 ± 1°C) under a 12:12 h light and dark cycle with free access to food and water. Each mouse was used for only one experiment. Experimental procedures were approved by the local ethical committee (IACUC) and conducted in accordance with international guidelines as well as European Communities Council Directive and National Regulations (CEE Council 86/609 and DL 116/92).

Nociceptive test

Nociception was evaluated by the radiant heat tail-flick test that consisted of the irradiation of the lower third of the tail with an I.R. source. Experiments were performed at room temperature (25 ± 1°C). The basal pre-drug latency was established between 3 and 4 s, which was calculated as the average of the first three measurements performed at 5 min intervals. A cut-off latency of 20 s was established to minimize damage to the tail. Post-treatment tail flick latencies (TFLs) were determined at 20, 30, 40, 60, 90 and 120 minutes after subcutaneous (s.c.) injection. Compounds under study were administered at the different doses (1.0, 2.0 and 5.0 mg/kg s.c.). Mice were pre-treated with those compoundsat 1 mg/kg s.c. 45 minutes prior morphine (4.0 mg/kg s.c.); tail flick latencies were measured after 20, 30, 40, 60, 90 and 120 minutes from the opioid administration. The behavioral tests were conducted by researchers blinded to treatment group.[66]

Statistical analysis

The data are expressed as mean ± SE. The inter-group comparisons were assessed using an initial two-way analysis of variance (ANOVA) followed by the Student's*t* test. Any differences were considered significant at $P < 0.05$.

Antiproliferative activity

Reagents. Trypan blue was purchased from Biochrom AG (Berlin, DE). Penicillin/streptomycin, trypsin, from Lonza (Verviers, BE). Fetal Calf Serum (FCS), medium 254 and Human Melanocyte Growth Supplement (HMGS) from GIBCO by Life Technologies (Grand Island, NY, USA). EMEM from ATCC (Manassas, VA, USA). For TUNEL assay In Situ Cell Death Detection Kit was purchased from ROCHE (Indianapolis, IN, USA). MTT and Siramesine were purchased from SIGMA-ALDRICH (St. Luis, MO,USA).

Cell Culture. Normal human melanocytes were prepared and maintained as described: the cells were grown in Medium 254 supplemented with 1% HMGS and penicillin/streptomycin (100 U/mL/50 µg/mL) under 5% CO_2 at 37°C. Informed consent was obtained from patients. Human melanoma cell lines SK-MEL-28 and SK-MEL-2 (from primary and metastatic melanoma, respectively) were bought from American Type Culture Collection (ATCC® HTB-72™, USA). The cells were cultured in EMEM supplemented with 10% FCS and penicillin / streptomycin (100 U/mL / 50 µg/mL) at 37°C and 5% CO_2.

*Evaluation of cytotoxic activity.*Cytotoxic effect of the tested compounds was evaluated by MTT dye test (cell viability). Normal human melanocytes, SK-MEL-2 and SK-MEL-28 were seeded in a 96-well culture plate at 15.000, 10.000 and 7.000 cells/well, respectively and incubated for 24 hours at 37°C to promote their adhesion. Then the culture medium was removed and increasing concentrations (20, 40, 80 and 100 µM) of the test compounds **1b**, **7b**, **10a**, **15b**, **16a**, **16b** and Siramesine were added to the wells and incubated without serum

for 24 and 48 hours. Untreated cells were used as viability control. After 24 and 48 hours, 20 µl of tetrazolium salt in PBS (5 mg/ml) were added to every well and the plates were incubated again for 4 hours. The medium was removed and the formazan salts, precipitated on the well bottom after oxidation, were dissolved with 200 µl of DMSO. The solubilized formazan was quantified with a microplate spectrophotometer at 540 nm wavelength, with reference at 690 nm. The results were expressed as viability percentage respect to the control. Results were calculated as the mean ± SD of three independent experiments performed in triplicate.[67]

Tunel assay. A standard protocol was provided by the manufacturer within the In Situ Cell Death Detection Kit. The cells were seeded in slide flasks at the density of 40.000, 36.000 and 27.000/cm^2 for normal human melanocytes, SK-MEL-2 and SK-MEL-28, respectively. The cells were incubated with 50 µL of the TUNEL kit for 1 hour at 37°C, in a humidified dark slide box. The ratio of apoptosis was examined under a fluorescence microscope (NIKON TE 2000) by counting positively stained cells in five different visual fields, selected randomly.

Statistical analysis

The data are expressed as mean ± SE. The inter-group comparisons were assessed by the Student's two-tailed *t* test. Any differences were considered significant at $P < 0.05$.

Acknowledgments

The authors would like to thank "Fondazione Cassa di Risparmio di Modena" (Pratica Sime n. 2015.0402) for financial support, Rossella Gallesi for elemental analysis, Nicola Fazio for helpful discussion and Johanna Chester for editorial assistance.

References

[1] W.R. Martin, C.G. Eades, J.A. Thompson, R.E. Huppler, P.E. Gilbert, *J. Pharmacol. Exp. Ther.* **1976,** *197*, 517-532.

[2] W.D. Bowen, *Pharm. Acta Helv.* **2000**, *74*, 211-218.

[3] S.B. Hellewell, W.D. Bowen, *Brain Res,* **1990**, *527*, 244-253.

[4] R. Quirion, W.D. Bowen, Y. Itzhak, J.L. Junien, J.M. Musacchio, R.B. Rothman, T.P. Su, S.W. Tarm, D.P. Taylor, *Trends Pharmacol. Sci.* **1992**, *13*, 85-86.

[5] M. Hanner, F.F. Moebius, A. Flandorfer, H.-G. Knaus, J. Striessnig, E. Kempner, H. Glossmann, *Proc. Natl. Acad. Sci. U.S.A.* **1996**, *93*, 8072-8077.

[6] R. Kekuda, P.D. Prasad, Y.J. Fei, F.H. Leibach, V. Ganapathy, *Biochem. Biophys. Res.* **1996**, *229*, 553-566.

[7] P. Seth, F.H. Leibach, V. Ganapathy, *Biochem. Biophys. Res. Commun.* **1997**, *241*, 535-540.

[8] Y.-X. Pan, J. Mei, J. Xu, B.-L. Wan, A. Zuckerman, G.W. Pasternak, *J. Neurochem,* **1998**, *70*, 2279-2285.

[9] P. Seth, Y.-J. Fei, H.W. Li, W. Huang, F.H. Leibach, V. Ganapathy, *J. Neurochem.* **1998**, *70*, 922-932.

[10] T.P. Su, E.D. London, J.H. Jaffe, *Science* **1988**, *239*, 219-221.

[11] C.P. Palmer, R. Mahen, E. Schnell, M.B.A. Djamgoz, E. Aydar, *Cancer Res.* **2007**, *67* 11166-11175.

[12] D. Fontanilla, M. Johannessen, A.R. Hajipour, N.V. Cozzi, M.B. Jackson, A.E. Ruoho, *Science* **2009**, *323*, 934-937.

[13] T.P. Su, *J. Pharmacol. Exp. Ther.* **1982**, *223*, 284-290.

[14] S.W. Tam, L. Cook, *Proc. Natl. Acad. Sci. U.S A.* **1984**, *81*, 5618-5621.

[15] W.D. Bowen, B.R. De Costa, S.B. Hellewell, J.M. Walker, K.C. Rice, *Mol. Neuropharmacol,* **1993**, *3*, 117-126.

[16] A. Cagnotto, A. Bastone, T. Mennini, *Eur. J. Pharmacol,* **1994**, *266*, 131-138.

[17] D.J. McCann, T.P. Su, D.J. McCann, T.P. Su, *Eur. J. Pharmacol.* **1990**, *188*, 211-218.

[18] S. Okuyama, Y. Imagawa, S.I. Ogawa, H. Araki, A. Ajima, M. Tanaka, M. Muramatsu, A. Nakazato, K. Yamaguchi, M. Yoshida, S. Otomo, NE-100, *Life Sci.* **1993**, *53*, PL285-290.

[19] S. Okuyama, A. Nakazato, NE-100: *CNS Drug Rev.* **1996**, *2*, 226-237.

[20] R. Bergeron, G. Debonnel, C. De Montigny, *Eur. J. Pharmacol.* **1993**, *240*, 319-323.

[21] K. Matsuno, T. Kobayashi, M.K. Tanaka, S. Mita, *Eur. J. Pharmacol.* **1996,** *312*, 267-271.

[22] A.D. Weissman, M.F. Casanova, J.E. Kleinman, E.D. London, E.B. De Souza, *Biol. Psychiatry* **1991,** *29*, 41-54.

[23] B. Wünsch, *J. Med. Chem.* **2012,** *55*, 8209-8210.

[24] J.L. Diaz, D. Zamanillo, J. Corbera, J.M. Baeyens, R. Maldonado, M.A. Pericas, J.M. Vela, A. Torrens, *Cent. Nerv. Syst. Agents Med. Chem.* **2009,** *9*, 172-183

[25] J.L. Diaz, R. Cuberes, J. Berrocal, M. Contijoch, U. Christmann, A. Fernandez, A. Port, J. Holenz, H. Buschmann, C. Laggner, M.T. Serafini, J. Burgeno, D. Zamanillo, M. Merlos, J.M. Vela, C. Almansa, *J. Med. Chem.* **2012,** *55*, 8211-8224.

[26] T. Maurice, T.P. Su, A. Privat, *Neuroscience* **1998,** *83*, 413-428.

[27] S. Collina, R. Gaggeri, A. Marra, A. Bassi, S. Negrinotti, F. Negri, D. Rossi, *Expert Opin. Ther. Pat.* **2013,** *23*, 597–613

[28] A. Marra, D. Rossi, L. Pignataro, C. Bigogno, A. Canta, N. Oggioni, A. Malacrida, M. Corbo, G. Cavaletti, M. Peviani, D. Curti, G. Dondio, S. Collina, *Future Med. Chem.* **2016,** *8*, 287-295.

[29] T. Maurice, T.P. Su, *Pharmacol Ther.* **2009,** *124,* 195-206.

[30] J. Xu, C. Zeng, W. Chu, F. Pan, J.M. Rothfuss, F. Zhang, Z. Tu, D. Zhou, D. Zeng, S. Vangveravong, F. Johnston, D. Spitzer, K.C. Chang, R.S. Hotchkiss, W.G. Hawkins, K.T. Wheeler, R.H. Mach, *Nat. Commun.* **2011,** *2:380* doi: 10.1038/ncomms1386.

[31] M.L. Pati, D. Groza,C. Riganti, J. Kopecka, M. Niso, F. Berardi, S. Hager, P. Heffeter, M. Hirai, H. Tsugawa, Y. Kabe, M. Suematsu, C. Abate, *Pharmacol Res.* **2017**, *117*, 67-74.

[32] A. Alon, H.R. Schmidt, M.D. Wood, J.J. Sahn, S.F. Martin, A.C. Kruse, *Proc. Natl. Acad. Sci. U S A* **2017**, *114,* 7160–7165.

[33] R.H. Mach, C.B. Zeng, W.G. Hawkins, *J. Med. Chem.* **2013,** *56*, 7137-7160.

[34] A. Van Waarde, A.A. Rybczynska, N. Ramakrishnan, K. Ishiwata, P.H. Elsinga, R.A. Dierckx, *Curr. Pharm. Des.* **2010,** 16, 3519–3537.

[35] K.W. Crawford, W.D. Bowen, *Cancer Res.* **2002,** *1*, 313-322.

[36] C. Zeng, J. Rothfuss, J. Zhang, W. Chu, S. Vangveravong, Z. Tu, F. Pan, K.C. Chang, R. Hotchkiss, R.H. Mach, *Br. J. Cancer.* **2012,** *106*, 693-701.

[37] N.A. Colabufo, F. Berardi, M. Contino, M. Niso, C. Abate, R. Perrone, V. Tortorella, *Naunyn Schmiedebergs Arch. Pharmacol.* **2004,** *370*, 106–113.

[38] M.A. Matos, A.P. Francisco, *ChemMedChem* **2013,** *8*, 1751-1765.

[39] S. Franchini, U.M. Battisti, A. Prandi, A. Tait, C. Borsari, E. Cichero, P. Fossa, A. Cilia, O. Prezzavento, S. Ronsisvalle, G. Aricò, C. Parenti, L. Brasili, *Eur. J Med. Chem.* **2016,** *112*, 1-19.

[40] T. Schlager, D. Schepmann, K. Lehmkuhl, J. Holenz, J. M. Vela, H. Buschmann, B. Wunsch, *J. Med. Chem.* 2011, *54*, 6704-6713.

[41] C. Oberdorf, D. Schepmann, J.M. Vela, H. Buschmann, J. Holenz, B. Wunsch, *J. Med.Chem.* 2012, *55*, 5350-5360.

[42] S. Franchini, U.M. Battisti, A. Baraldi, A. Prandi, P. Fossa, E. Cichero, A. Tait, C. Sorbi, G. Marucci, A. Cilia, L. Pirona, L. Brasili, *Eur. J. Med.Chem.* **2014,** *87,* 248-266.

[43] S. Franchini, L.I. Manasieva, C. Sorbi, U.M. Battisti, P. Fossa, E. Cichero, N. Denora, R.M. Iacobazzi, A. Cilia, L. Pirona, S. Ronsisvalle, G. Aricò, L. Brasili, *Eur J. Med. Chem.* **2016**, *125*, 435-452.

[44] S. Franchini, A. Prandi, C. Sorbi, A. Tait, A. Baraldi, P. Angeli, M. Buccioni, A. Cilia, E. Poggesi, P. Fossa, L. Brasili, *Bioorg. Med. Chem. Lett.* **2010,** *20*, 2017–2020.

[45] C. Sorbi, S. Franchini, A. Tait, A. Prandi, R. Gallesi, P. Angeli, G. Marucci, L. Pirona, E. Poggesi, L. Brasili, *ChemMedChem* **2009,** *4*, 393–399.

[46] A. Prandi, S. Franchini, L.I. Manasieva, P. Fossa, E. Cichero, G. Marucci, M. Buccioni, A. Cilia, L. Pirona, L. Brasili, *J. Med. Chem.* **2012,** *55*, 23–36.

[47] Y.-C. Cheng, W.H. Prusoff, *Biochem. Pharmacol.* **1973,** *22*, 3099-3108.

[48] E. Laurini, D. Marson, V. Dal Col, M. Fermeglia, M.G. Mamolo, D. Zampieri, L. Vio, S. Pricl, *Mol. Pharm.* **2012,** *9*, 3107-3126.

[49] C. Meyer, D. Schepmann, S. Yanagisawa, J. Yamaguchi, V. Dal Col, E. Laurini, K. Itami, S. Pricl, B. Wünsch, *J. Med. Chem.* **2012,** *55*, 8047-8065.

[50] S. Brune, D. Schepmann, K.H. Klempnauer, D. Marson, V. Dal Col, E. Laurini, M. Fermeglia, B. Wünsch, S. Pricl, *Biochemistry* **2014,** *53*, 2993-3003.

[51] H.R. Schmidt, S. Zheng, E. Gurpinar, A. Koehl, A. Manglik, A.C. Kruse, *Nature* **2016,** *532*, 527-530.

[52] G.W. Pasternack, *σ1 Receptors and the Modulation of Opiate Analgesics. In Sigma Receptors: Chemistry, Cell Biology and Clinical Implications*; Kluwer Academic Publishers, New York, **2006**, p. 337.

[53] A. Vidal-Torres, B. de la Puente, M. Rocasalbas, C. Touriño, S.A. Bura, B. Fernández-Pastor, L. Romero, X. Codony, D. Zamanillo, H. Buschmann, M. Merlos, J.M. Baeyens, R. Maldonado, J.M. Vela, *Eur. J. Pharmacol.* **2013,** *711*, 63-72.

[54] H. Sun, M. Shi, W. Zhang, Y.M. Zheng, Y.Z. Xu, J.J. Shi, T. Liu, H. Gunosewoyo, T. Pang, Z.B. Gao, F. Yang, J. Tang, L.F. Yu, *J. Med. Chem.* **2016,** *59*, 6329−6343.

[55] J. M. Entrena, E. J. Cobos, F. R. Nieto, C. M. Cendán, G. Gris, E. Del Pozo, D. Zamanillo, J. M. Baeyens, *PAIN*, **2009**, *143*, 252–261.

[56] F. Xie, T. Kniess, C. Neuber, W. Deuther-Conrad, C. Mamat, B.P. Lieberman, B. Liu, R.H. Mach, P. Brust, J. Steinbach, J. Pietzsch, H. Jia, *Med. Chem. Commun.* **2015,** *6*, 1093-1103.

[57] C. Zeng, J.M. Rothfuss, J. Zhang, S. Vangveravong, W. Chu, S.Li, Z. Tu, J. Xu, R.H. Mach, *Anal. Biochem.* **2014,** *448*, 68-74.

[58] M.H. Česen, U. Repnik, V, Turk, B. Turk, *Cell Death and Dis.* **2013,** *4*, e818.

[59] M.S. Ostenfeld, N. Fehrenbacher, M. Høyer-Hansen, C. Thomsen, T. Farkas, M. Jäättelä, *Cancer Res.* **2005,** *65*, 8975-8983.

[60] R.R. Matsumoto, W.D. Bowen, M.A. Tom, V.N. Vo, D.D. Truong, B.R. De Costa, *Eur. J. Pharmacol.* **1995,** *280*, 301−310.

[61] D.L. DeHaven-Hudkins, Y. Ford-Rice, *Eur. J. Pharmacol.* **1992,** *227*, 371−378.

[62] R.H. Macth, C.R. Smith, S.R. Childers, *Life Sci.* **1995,** *57*, 57−62.

[63] R. Testa, L. Guarneri, E. Poggesi, P. Angelico, C. Velasco, M. Ibba, A. Cilia, G. Motta, C. Riva, A. Leonardi, *J. Pharmacol. Exp. Ther.* **1999,** *290*, 1258–1269.

[64] P. Fossa, E. Cichero, *Bioorg. Med. Chem.* **2015,** *23*, 3215-3220.

[65] V. Deiana, M. Gómez-Cañas, M.R. Pazos, J. Fernández-Ruiz, B. Asproni, E. Cichero, P. Fossa, E. Muñoz, F. Deligia, G. Murineddu, M. García-Arencibia, G.A. Pinna, *Eur. J. Med. Chem.* **2016,** *112*, 66-80.

[66] O. Prezzavento, C. Parenti, A. Marrazzo, S. Ronsisvalle, F. Vittorio, G. Aricò, G.M. Scoto, G. Ronsisvalle, *Life Sci.* **2008,** *82*, 549-553.

[67] T. Mosmann, *J. Immunol. Methods,* **1983,** *65*, 55-63.

Table of Contents Entry

Structural modifications of the starting compounds **1a** / **1b** allowed to disclose a new series of spiro-cyclic σR ligands. Among them, the most interesting are:

- **15b** and **16b** for their agonist and antagonist activity at σ_1R, respectively;
- **16a** for its selective toxicity towards SK-Mel-2 metastatic melanoma cell lines versus SK-Mel-28 and melanocytes, suggesting an agonistic behavior at σ_2R.

Docking studies were performed on the theoretical σ_1R homology model.